Gold recovery from precious metals in acidic media by using human hair waste as a new pretreatment-free green material

Dan Yu [a], Shintaro Morisada [a], Hidetaka Kawakita [a], Koichi Sakaguchi [a], Satoshi Osada [a],
Keisuke Ohto [a,*], Katsutoshi Inoue [a], Xi-Ming Song [b], Guolin Zhang [b],
Ramachandra Rao Sathuluri [a,c]

[a] *Department of Chemistry and Applied Chemistry, Saga University, 1-Honjo, Saga 840-8502, Japan*
[b] *College of Chemistry, Liaoning University, Shenyang 110036, China*
[c] *Department of Reproductive Biomedicine, The National Institute of Health and Family Welfare, Munirka, New Delhi 110067 India*

ARTICLE INFO

ABSTRACT

We herein propose an advanced gold recovery process employing biomass waste of human origin. Au(III) adsorption on human hair (HH) was found to be efficient and to concurrently reduce Au(III) to metallic gold. The maximum loading capacities of gold on HH and white HH were determined using Langmuir equation fitting to be 3.04 and 3.24 mmol g^{-1}, respectively. This result indicates that melanin pigment in HH is not involved in Au(III) adsorption. The concurrent reduction of Au(III) was confirmed using X-ray diffraction analysis and scanning electron microscopy before and after Au(III) adsorption. To gain more detailed understanding of Au(III) adsorption at a molecular level, complexations of Au(III) with each amino acid component found in the peptides of HH was investigated. L-Cystine and L-cysteine were found to play a role in both the adsorption and reduction of Au(III). The mechanism of Au(III) adsorption and reduction on HH was investigated using proton nuclear magnetic resonance spectroscopy. The stepwise purification of three precious metals was also demonstrated: Pt (IV) and Pd(II) were successfully removed from HH by washing with acidic thiourea solution, while pure gold could be recovered by incineration. Thus, HH waste has shown potential as beneficial and efficient utilization on the separation and recovery of precious metals.

1. Introduction

Precious metals are valued for their application in a wide array of modern industries, including electronics, catalysts, medicines, and jewelry. Rapid technological innovation has accelerated the consumption of precious metals and resulted in the production of huge quantities of electronic waste. The accumulation of electronic waste in 2016 was reached to 7211 kilotons (kt) in China, 6295 kt in U.S., 2139 kt in Japan and 1884 kt in Germany [1]. Although precious metals take a seemingly small content in electronic devices (< 0.5 %), they have decisive impact of the value of electronic scrap [2]. Only computer equipment and mobile phones take 3 % share of the world production for Ag, 4 % of Au and 16 % of Pd production [3]. These domestic metal wastes represent a significant untapped resource. This "urban mine" contains various metals at minute concentrations within a vast quantity of non-metallic materials [4], so highly specific selectivity is required for the separation and recovery of precious metals.

After multistep of physical pre-separation for non-metallic parts removal, hydrometallurgical technology, is generally utilized for the stepwise separation and recovery of precious metals from leaching solutions [5]. It has been achieved with various techniques, including precipitation, solvent extraction, adsorption and electrolysis. Classical precipitation methods are most extensively applied at the early stages of stepwise separation, such as silver removal [6,7]. Isolation of individual metals at the latter stages is often achieved with the use of extractants and adsorbents, owing to their high capacity and specific selectivity for metal separation [8,9]. The adsorption technique avoids the use of flammable organic solvents required in the solvent extraction process. Among various kinds of adsorbents, those prepared from biomass waste are attractive for their low cost, ease of preparation and environmental friendliness. Bio-adsorbents use various functional groups, including amino, hydroxyl, carboxylic acid and carbonyl moieties, to facilitate

metal adsorption via complexation or chelation [10].

Bio-adsorbents sourced from biomass waste can be classified on the basis of active component into materials rich in polysaccharides, proteins or polyphenols. Polysaccharides have alcoholic hydroxyl groups, proteins consist of various amino acids and polyphenols use phenolic hydroxyl groups. To date, plant leaves [11,12], crustacean shells [13], eggshell membranes [14], and fruit peels [15], have been employed as bio-adsorbents for precious metals with remarkable capacities. In this work, we have investigated the use of human hair (HH) waste as a protein-rich adsorbent for Au(III) recovery. Most bio-adsorbents are environmentally friendly, but often suffer from easy deterioration and limited shelf life. HH waste has more than environmentally friendly property with mold-resistance.

HH is naturally derived and abundant, with annual production approximated at 5.9 kt in 2011 (roughly estimated from the reported amount of HH produced in India in 2011, extrapolated from the ratio between Indian and global population in 2011) [16,17]. HH comprises 65 %–95 % protein with the remainder comprising water, lipids, polysaccharides, pigments, nucleic acids, and trace elements [18]. Research using HH has been undertaken in the fields of cosmetics, medical science, and chemical materials [19–21]. Complete hydrolysis of the protein in HH reveals that it contains 13 %–18 % cysteine [22], which stabilizes the structure of HH from weathering and exposure to reducing, oxidizing, and hydrolyzing reagents. Cystine, the dimer of cysteine exists in cuticle layer and contributes to high wet strength, moderate swelling, and insolubility [23]. Proteins in HH are densely cross-linked by cystine disulfide bonds. Cysteine and cystine are sulfur-containing and typically classified as soft Lewis bases with high affinity for soft acids such as gold [24,25]. L-Cysteine adsorption onto the surface of gold via an Au-S bond has been reported [26,27].

HH waste is an abundant biomass resource that boasts excellent stability and unique chemical properties. We have focused herein on the application of untreated HH waste in the adsorption and separation of precious metals. Both white human hair (WHH) and black HH were evaluated for gold adsorption to ascertain the role of melanin. Selectivity for gold over other precious metal ions, recovery after adsorption and incineration were also investigated. Proton nuclear magnetic resonance spectroscopy was carried out to elucidate the mechanism of gold adsorption on HH.

2. Materials and methods

2.1. General procedures

The concentrations of precious metals in sample solutions were measured using an inductively coupled plasma atomic emission spectrometer (ICP-AES; Shimadzu, ICPS-8100). The structure of the samples was assessed using X-ray diffraction (XRD; Shimadzu, XRD-7000). The images were collected on a digital microscope (KEYENCE, VHX-1000). The micrographs were taken using scanning electron microscopy (SEM; Hitachi, SU-I500). Elemental analysis of the samples was carried out using energy dispersive spectroscopy (EDS; Hitachi, SU-8010). Proton nuclear magnetic resonance (^{1}H NMR) spectra were obtained on an NMR spectrometer (400 MHz, Agilent). Metallic gold was obtained via incineration of Au-loaded HH in muffle furnace (Yamato model FO100). EDS spectra were measured with the support of Liaoning University, while all other equipment was accessed at the Analytical Research Center for Experimental Sciences of Saga University.

2.2. Reagents

Precious metals (gold(III), platinum(IV), palladium(II), and silver(I)) solutions were prepared by dissolving appropriate amounts of hydrogen tetrachloroaurate(III) tetrahydrate (HAuCl$_4$·4H$_2$O), hydrogen hexachloroplatinate(IV) hexahydrate (H$_2$PtCl$_6$·6H$_2$O), palladium(II) nitrate, and silver nitrate salts, respectively, in acidic solutions. All metal salts,

as well as hydrochloric acid, nitric acid, ethanol, and amino acids (L-cysteine, L-cystine, L-alanine, glycine, L-glutamic acid and L-serine), were purchased from Wako Pure Chemical Industries, Ltd, Osaka, Japan. L-Arginine was purchased from SIGMA-Aldrich, USA. Crude HH was supplied by a barbershop in Saga, Japan. Deuterium oxide (D$_2$O) and hydrogen peroxide (H$_2$O$_2$) were procured from SIGMA-Aldrich, USA. Deuterium chloride (DCl, 35 % solution in 99.5 % D$_2$O) was purchased from Wako Pure Chemical Industries.

2.3. Method for adsorbent preparation

The supplied HH was cut to approximately 0.3–1 mm lengths. Cut HH (3.0 g) was stirred in ethanol (100 mL) for 1 h to wash out impurities (oil, dust, scurf) and stood overnight. The washed HH was then dried at room temperature and stored out of direct sunlight. Clean HH with or without gold loading was analyzed using EDS, XRD, and SEM. Although the "untreated HH" is often used for the obtained HH in this article, it was used as bio-adsorbent.

2.4. Precious metal adsorption in acidic media

Precious metal adsorption on HH was carried out using a conventional batch-wise method from two acidic aqueous media: nitric acid and hydrochloric acid (except with silver, because of precipitation of silver chloride). Metal solutions were prepared by dissolving each metal salt 1.0 mM (M = mol/L) in acidic solution (10 mL). HH or WHH (20 mg) was added to each metal solution (1.0 mM) and adsorption was carried out at 30°C with 150 rpm shaking for 24 h. After filtration, the metal concentration of the aqueous solution was measured using ICP-AES. Time dependence of individual precious metal adsorption was assessed using 0.10 M HNO$_3$ with different shaking time intervals. Maximum adsorption capacity was tested by varying metal concentration in 0.10 M HNO$_3$. The gold-loaded adsorbents were analyzed using SEM, digital microscope, and XRD. For the recovery test, directly after the competitive adsorption test, the metal loaded HH (1.0 g) was washed 3 times with deionized water (3 × 300 mL) followed by washing with acidic thiourea (0.05 M in 0.01 M HCl, 300 mL) at 30°C with different shaking time intervals at 150 rpm. The concentration of eluted metal in the sample solution was measured using ICP-AES.

The adsorption percentage was calculated using Eq. (1):

$$\%Adsorption = \frac{C_i - C_e}{C_i} \times 100 \tag{1}$$

the amount of metal adsorbed per unit mass of the adsorbents was calculated using Eq. (2):

$$q = \frac{C_i - C_e}{W} \times V_M \tag{2}$$

and the elution percentage from the HH was calculated using Eq. (3):

$$\%Elution = \frac{\eta_E}{\eta_{Ad}} \times 100 \tag{3}$$

where C_i and C_e are the initial and equilibrium concentrations (mM) of metal ions, respectively; V_M is the volume (L) of sample solution; W is the weight (g) of adsorbent; and η_E and η_{Ad} are the eluted and adsorbed molar quantities of gold (mmol), respectively.

2.5. Au(III) complexation with various amino acids

Each amino acid (22.0 μmol), L-cystine, L-cysteine, L-serine, L-glutamic, glycine, L-arginine and L-alanine, was dissolved in 10 mL of 0.10 M HNO$_3$ solution containing 1.0 mM Au(III). The mixture was shaken at 150 rpm at 30°C for 24 h. Because of precipitate formation, the samples were passed through a 0.45-μm membrane filter and the metal concentration in the filtrate was measured using ICP-AES. For ^{1}H NMR
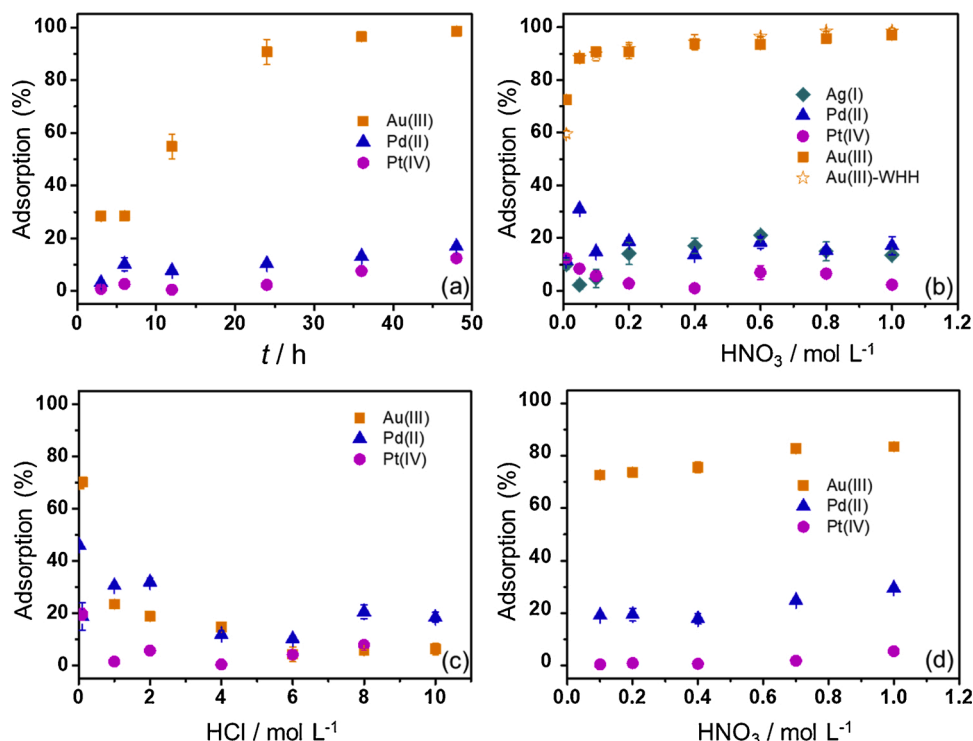
Fig. 1. (a) Time dependence of individual system of adsorption on HH in 0.10 M HNO$_3$, effect of (b) nitric and (c) hydrochloric acids concentration on adsorption percentage of precious metals on HH in individual system, (d) nitric acid in competitive system.

measurements, L-cystine (1.00 mg, 4.16 μmol) or L-cysteine (1.00 mg, 5.69 μmol) was dissolved into 1.0 mL D$_2$O containing a trace DCl. The solution was then mixed with HAuCl$_4$·4H$_2$O (45.0 mg, 109 μmol) to form a gold complex. The spectra of cystine and cysteine were obtained at two time intervals (1 min, 1 h) before and after complexation with gold. In a subsequent experiment, cysteine (20.0 mg, 114 μmol) was dissolved in 0.4 mL D$_2$O containing a trace DCl and mixed with 0.4 mL H$_2$O$_2$. The spectra were obtained at two time intervals (1 min, 168 h) post peroxide addition.

2.6. Recovery of metallic gold from HH

To recover pure gold after the adsorption of mixed precious metals, the HH was washed thrice with deionized water and once with acidic thiourea (0.05 M in 0.01 M HCl) before incineration in the muffle furnace at 800 °C for 2 h.

3. Results and discussion

3.1. Time dependence of precious metal adsorption on HH

The time dependence of Au(III), Pd(II) and Pt(IV) adsorption on HH in 0.10 M HNO$_3$ is shown in Fig. 1a. Au(III) adsorption on HH gradually increased over time and reached a plateau after 24 h. Pd(II) and Pt(IV) adsorption on HH also increased gradually over time, although the increase in adsorption percentage was too small to be significant. The optimal time for precious metal adsorption on HH was determined to be 24 h.

3.2. Precious metal adsorption in individual and competitive systems

Precious metal adsorption on HH in individual and competitive systems was investigated. To confirm the role of melanin in Au(III) adsorption, WHH was also studied. The effect of nitric acid concentration on the adsorption percentage of precious metals on HH and WHH in
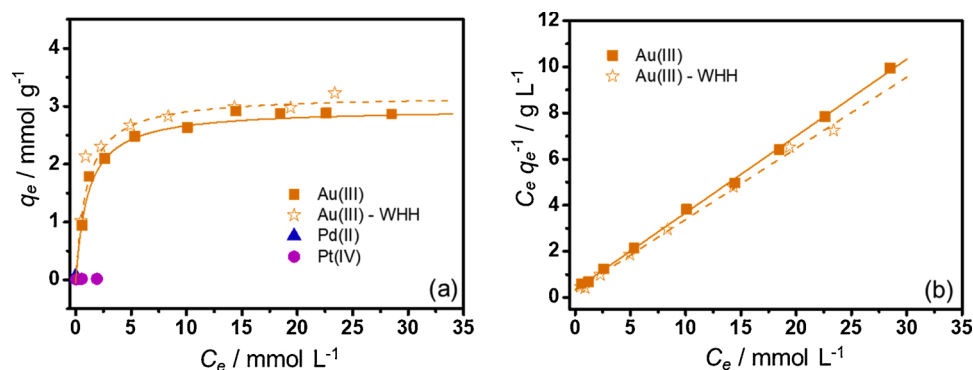
Fig. 2. (a) Adsorption isotherm of precious metals on HH and Au(III) on WHH in 0.10 M HNO$_3$, (b) The Langmuir isotherm kinetic model of Au(III) adsorption on HH and WHH in 0.10 M HNO$_3$.

the individual system is shown in Fig. 1b. Results showed a marked increase in Au(III) adsorption on HH and WHH with the increasing nitric acid concentration up to 0.05 M. The Au(III) adsorption percentage then plateaued and increased only marginally between 0.05 and 0.2 M nitric acid. The adsorption percentage at 24 h of Ag(I), Pd(II) and Pt(IV) on HH was less than 20 % regardless of the concentration of nitric acid. The increase in Au(III) adsorption with increasing nitric acid concentration reveals that adsorption is remarkably sensitive to acid strength, particularly for concentrations < 0.05 M nitric acid. Comparison of the adsorption between WHH and HH suggests that melanin is not involved in the binding mechanism.

The effect of hydrochloric acid concentration on the adsorption percentage of precious metals on HH in the individual system is shown in Fig. 1c. Au(III) adsorption on HH was markedly suppressed with increasing hydrochloric acid concentration, likely as a result of the conversion of free Au^{3+} to $AuCl_4^-$ [28,29]. Pd(II) adsorption, however, was not significantly suppressed, possibly indicating a mechanism of adsorption different from Au(III). Pt(IV) adsorption was negligible regardless of the concentration of hydrochloric acid (Fig. 1c).

Precious metal adsorption on HH in a competitive system was investigated next. The effect of nitric acid concentration on the adsorption percentage of precious metals on HH in the competitive system is shown in Fig. 1d. Relative to the individual system, Au(III) adsorption on HH was diminished by the adsorption of other precious metals and coexisting chloride ions from the Pt(IV) salt. High selectivity for Au(III) over Pd(II) and Pt(IV) was still observed.

3.3. Adsorption isotherm of precious metals on HH and WHH

3.3.1. Langmuir isotherm model

The individual adsorption isotherm for precious metal ions on HH and WHH in 0.10 M HNO_3 are shown in Fig. 2a. The amount of Au(III) adsorbed on HH increased in line with the equilibrium concentration of Au(III) before reaching the maximum adsorption capacity, which follows a typical Langmuir adsorption model [30]. The maximum adsorption capacity of HH and WHH for Au(III) reached over 3 mmol g^{-1}. However, the adsorption capacity of HH for Pd(II) was less than 0.1 mmol g^{-1} and Pt(IV) was negligible.

The adsorption capacities of HH and WHH for Au(III) were calculated using the Langmuir model, represented by Eq. (4):

$$q_e = \frac{q_m K_L C_e}{1 + K_L C_e} = \frac{q_m C_e}{1/K_L + C_e} \tag{4}$$

where q_e and q_m are the adsorption amount at equilibrium (mmol g^{-1}) and the maximum adsorption capacity (mmol g^{-1}), respectively; the term "K_L" is the Langmuir constant related to the adsorption energy (L $mmol^{-1}$). When equilibrium concentration, C_e, is greater than the value of $1/K_L$, the maximal adsorption capacity is obtained.

To further confirm the validity of the maximum adsorption capacities, Eq. (4) was converted:

$$\frac{C_e}{q_e} = \frac{1}{q_m K_L} + \frac{C_e}{q_m} \tag{5}$$

Eq. (5) depicts a linear relationship between $C_e\, q^{-1}$ and C_e for Au(III) adsorption on both HH and WHH. Based on Eq. (5), the converted Langmuir adsorption isotherms of Au(III) on HH and WHH were obtained as shown in Fig. 2b. The regression coefficient (R^2) values for both are > 0.99. Valid adsorption capacity for Pd(II) was evaluated by Eq. (5) as well. Langmuir parameters and the maximum adsorption capacities of precious metals were calculated from the slope and intercept using linear regression analysis and are shown in Table S1. Adsorption capacity of HH for Pd(II) (0.071 mmol g^{-1}) was much lower than that for Au(III) (3.04 mmol g^{-1}). This result suggests that the adsorption percentages for Pd(II) and Pt(IV) (depict in Fig. 1) were the product of a physical process, rather than chemical affinity. WHH possess

Table 1

Langmuir and Freundlich isotherm parameter values for Au(III) adsorption on human hair (HH) and white human hair (WHH).[a]

Adsorbent	Langmuir isotherm model			Freundlich isotherm model		
	q_m (mmol g^{-1})	K_L (L $mmol^{-1}$)	R^2	K_F (mmol g^{-1})/ (mmol L^{-1})$^{1/n}$	n	R^2
HH	3.04	0.960	0.9995	1.742	5.22	0.981
WHH	3.24	0.994	0.9984	2.118	8.21	0.939

[a] q_m = maximum adsorption capacity; K_L/K_F = Langmuir/Freundlich constant; R^2 = linear regression coefficient.

Table 2

Au(III) adsorption capacities of human hair (HH) and white human hair (WHH) relative to previously characterized bio-adsorbents.

Adsorbent	Au(III) Adsorption Capacity (q_m) (mmol g^{-1})	pH_i	Time to reach plateau/h	References
Silk sericin	1.0	2.4−2.55	–	[31]
Eggshell membrane	3.13	3	2	[32]
Modified Lagerstroemia speciosa leaves (PEI-LS)	1.52	1	6	[33]
Modified cellulose (TDAC)	0.175	3.26	24	[34]
Raw date pits	0.396	0.3	2	[35]
Modified wood powder	4.31	0	4	[36]
Calcium alginate	1.47	2	24	[37]
Human hair (HH)	3.04	1	24	Present work
White human hair (WHH)	3.24	1	–	Present work

comparable adsorption capacity (3.24 mmol g^{-1}) to HH. The slight difference in adsorption capacity between HH and WHH may be caused by differing amounts of active functional group per unit weight of hair.

3.3.2. Freundlich isotherm model

The adsorption isotherm of Au(III) on HH and WHH was studied by Freundlich model as well. The linearized forms of Freundlich isotherm was expressed by the Eq. (6):

$$\log q_e = \log K_F + n^{-1}\log C_e \tag{6}$$

where K_F and n represent Freundlich isotherm constant and adsorption intensity. The isotherms of Au(III) adsorption on HH and WHH are shown in Fig. S1. The values of K_F and n were calculated from the intercept and slope of the linear plot between log q_e and log C_e were listed in Table 1. It is well known that the adsorption process is favorable by the range of n value between 1–10, and the higher values stands for the stronger adsorption intensity. Comparison of R^2 values between Langmuir and Freundlich isotherm models (Table 1) indicated that Langmuir isotherm model is an excellent fit to the experimental data.

Additionally, the Au(III) adsorption capacities of HH and WHH are compared with other biomass materials in Table 2 [31–37]. Untreated biomass waste WHH and HH exhibit capacity of Au(III) adsorption is comparable to the modified materials or superior to previously characterized raw bio-adsorbents, although it taking longer time to reach maximum capacity. It reveals adequately high application for the future.

3.4. The oxidation state of Au after adsorption on HH

We have reported in previous work that adsorbents derived from biomass waste containing polyphenols, pectic acid and cellulose not
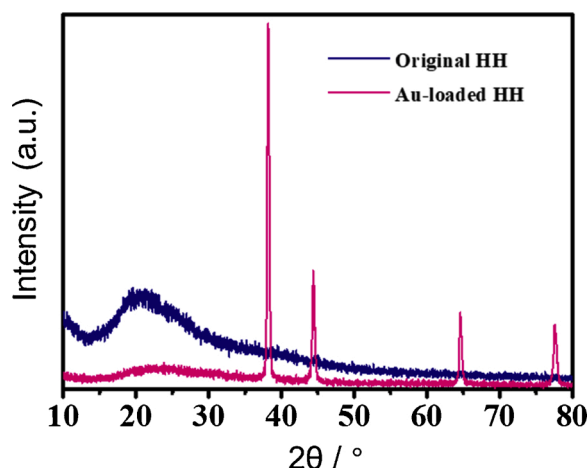
Fig. 3. XRD patterns of original HH and Au-loaded HH (1.07 mmol g^{-1}).

only adsorb Au(III) but also reduce it to its metallic state [38–42], so we suspected that HH may also be capable of the concurrent reduction of Au (III). To confirm the oxidation state of Au after the adsorption on HH, the XRD analysis of Au-loaded HH was carried out. The XRD patterns before and after Au-loading are shown in Fig. 3. The pattern of the original HH shows only a broad peak at around 21° as 2θ value, while the sharp peaks of Au-loaded HH were observed at 38.29°, 44.39°, 64.74°, and 77.62°. These peaks correspond to those of metallic gold reported by our group and other researchers [38–42,43]. The crystalline peaks demonstrate that the concurrent reduction of Au(III) on HH does indeed take place during the adsorption.

3.5. Characterization of HH and Au-loaded HH

After the reduction of Au(III) on HH was confirmed, the surface morphologies and the surface elemental analysis of the HH before and after Au(III) adsorption were measured using SEM, digital microscope and EDS.

3.5.1. Surface morphology of HH before and after Au(III) adsorption

The SEM and microscope images of the original HH, Au-loaded HH and the cut cross-section surface of the Au-loaded HH are shown in Fig. 4a-d. Images of Au-loaded HH at both low (0.493 mmol g^{-1}) and high (2.881 mmol g^{-1}) levels of adsorption were obtained. Because the supplied hair was used without treatment or selection, variation in diameter can be observed (Fig. 4a). Visible aggregates of gold particles after adsorption appear as white spots at the outermost layer of the HH (Fig. 4b). The visualization of gold particles further confirms the XRD data (Fig. 3). Interestingly, gold particles were not observed at the cut cross-section surface of the Au-loaded HH (Fig. 4c). This result indicates that gold particles are not bound at the inner layers of HH, the adsorption reduction take place exclusively at the surface. Gold particles were observed at the surface of WHH in a similar fashion (Figs. 4d and S2). This result further confirms that the capacity and mechanism of adsorption are the same for WHH and HH. Increased coverage area can be observed when comparing of the Au-loaded HH at low and high levels of adsorption (Fig. 4b and d).

3.5.2. Surface elemental analysis of HH before and after Au(III) adsorption

EDS analysis was carried out to investigate changes in the elemental composition on the surface of HH. Untreated HH, HNO$_3$-treated HH and Au-loaded HH were evaluated. The results are shown in Fig. 5a–c; Fig. S3 shows 0.1 M HCl-treated HH. The average atomic percentages of sulfur and gold on the untreated HH were 0.67 % and 0.03 %, respectively. After treatment with 0.10 M HNO$_3$ or 0.10 M HCl, the average atomic percentages of sulfur increased to 1.97 % and 2.13 %, respectively. This demonstrates that treatment with acid frees sulfur-containing components on the surface of HH. A strong peak corresponding to atomic Au was observed after Au adsorption, and atomic percentage increased to 11.67 % (Fig. 5c). The average atomic percentage of sulfur after Au adsorption decreased only modestly to 1.46 %. Sulfur-containing components may affect Au(III) adsorption and
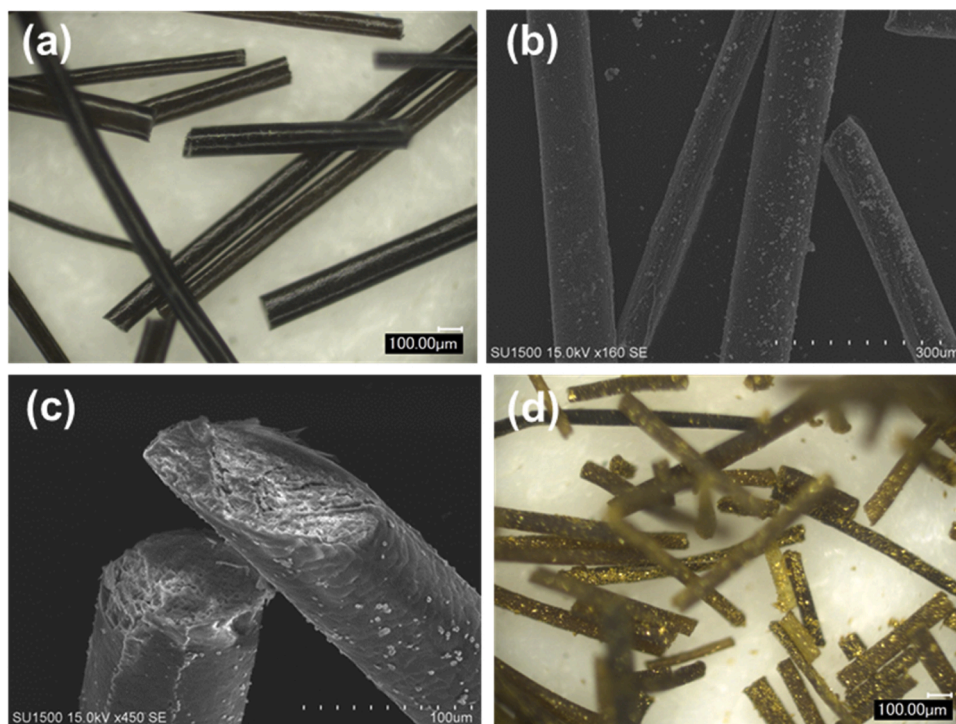

Fig. 4. SEM and microscope images of HH before and after Au(III) adsorption: (a) untreated HH, (b) Au-loaded HH (0.493 mmol g^{-1}), (c) the cut cross-section of Au-loaded HH, (d) Au-loaded HH (2.881 mmol g^{-1}).
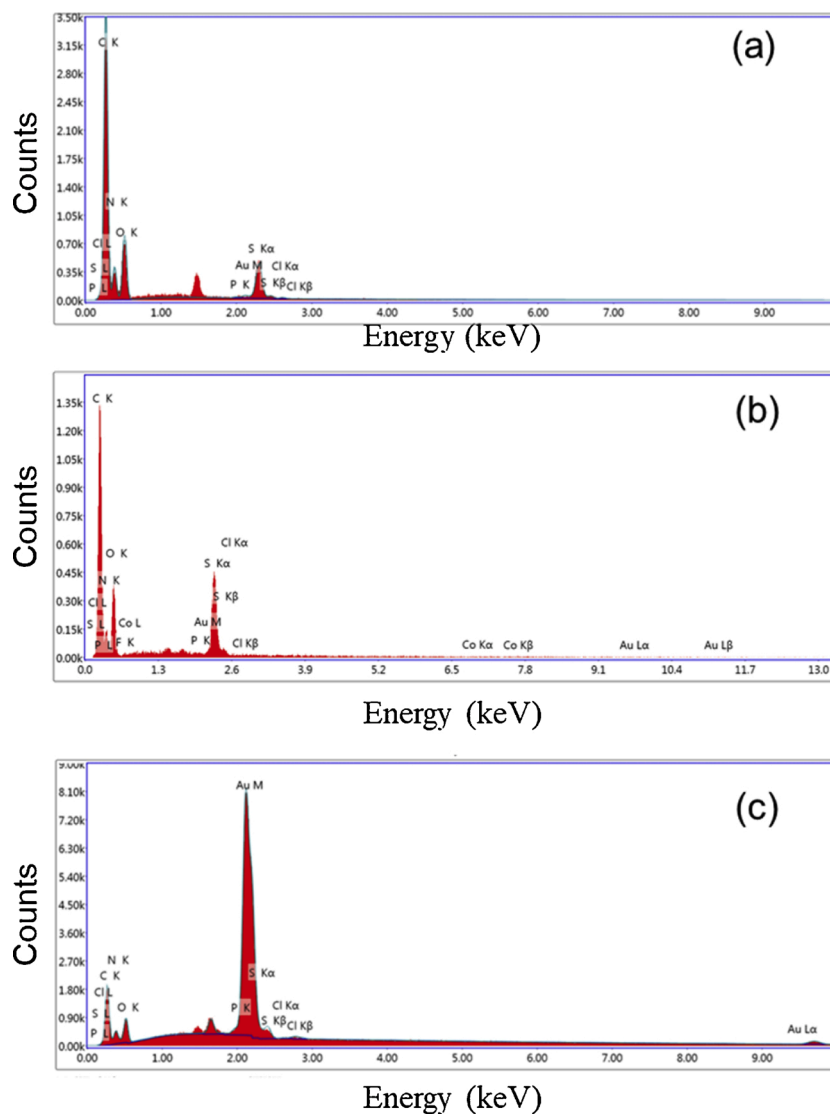
Fig. 5. EDS analyses of (a) untreated HH, (b) 0.10 M HNO$_3$-treated HH, (c) Au-loaded HH.

reduction.

HH is layered and comprises the medulla, cortex and cuticle. The cuticle is the outermost layer and comprises the epicuticle, A-layer, exocuticle, endocuticle and inner layer. Sulfur-containing cystine is found primarily in the A-layer (35 %) and exocuticle (15 %). Moreover, cystine is the oxidized dimer of the monomer, cysteine. After protein hydrolysis, cysteine is the most abundant amino acid in HH [44]. The sulfur-containing components detected using EDS are therefore very likely to be related to cystine and cysteine.

3.6. Mechanism of Au adsorption on HH

3.6.1. Au(III) complexation with various amino acids

The role of cysteine and cystine, as well as other constituent amino acids in HH, on Au adsorption was further investigated. The amino acid present in HH is as follows: L-cysteine (17.5 %), L-serine (11.7 %), L-glutamic acid (11.1 %), glycine (6.5 %), L-arginine (5.6 %) and L-alanine (4.8 %) [44]. The complexation of Au(III) with each of these amino acids was studied. To approximate amino acid concentration in a sample of HH bio-adsorbent (estimated from cysteine as 0.029 mmol per 20 mg HH), a quantity of 0.022 mmol of each amino acid was individually employed. The formation of a precipitate was occasionally observed upon dissolution of each amino acid in 0.10 M HNO$_3$ containing 1.0 mM
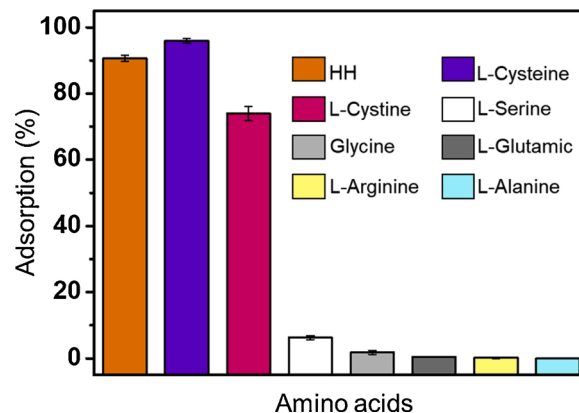

Fig. 6. Individual complexation of Au(III) with various amino acids in 0.10 M HNO$_3$.

Au(III). Au concentration was determined after filtration. Results for the complexation of Au(III) with various individual amino acids in nitric acid solution are shown in Fig. 6. Cysteine and cystine were found to achieve far more extensive complexation with Au(III) relative to the
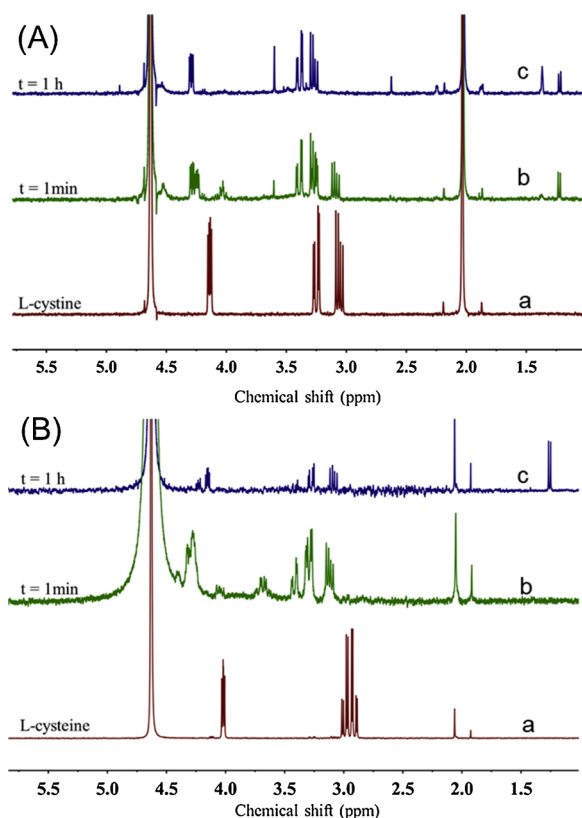
Fig. 7. ¹H NMR spectrum of (A) ʟ-cystine in D₂O-DCl (a), Au(III) mixture (1 min) (b), Au(III) mixture (1 h later) (c); (B) ʟ-cyteine in D₂O-DCl (a), Au(III) mixture (1 min) (b), Au(III) mixture (1 h later) (c).

other amino acids investigated; their performance in Au adsorption was even comparable to HH. ʟ-Serine, which has a primary hydroxyl group, also displayed significant complexation ability. However, little or no complexation with Au(III) was observed for the other amino acids investigated. These results suggest that amide carbonyl groups are not effective moieties for Au complexation while the sulfur atoms in cysteine and cystine display a high affinity for gold. We concluded from this work that it is highly probable that the sulfur-containing components detected using EDS are cysteine and cystine, and further suspected that the oxidation of cysteine to cystine may be related to the reduction of Au(III) to metallic gold. Further investigation was carried out to elucidate the mechanism.

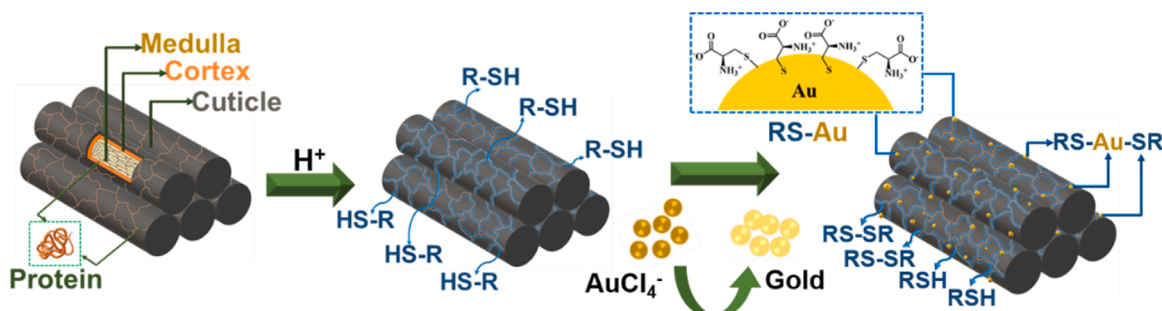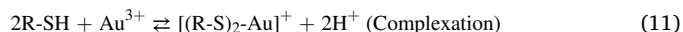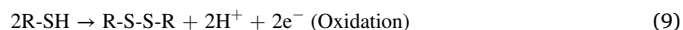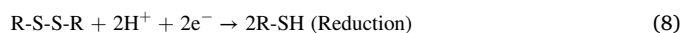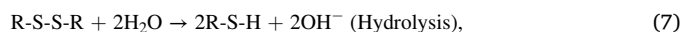### 3.6.2. ¹H NMR spectra of cystine and cysteine before and after reaction with Au(III)

The ¹H NMR spectra of cystine and cysteine in D₂O–DCl solution before and after exposure to Au(III) were obtained. Spectra were obtained at two timepoints: 1 min and 1 h after reaction with Au(III). The

¹H NMR spectra of cystine, cysteine, and their Au(III) complexes are shown in Fig. 7A and B. Because of their position adjacent to a chiral center, the methylene protons of cystine appear as a doublet of doublets at 3.00–3.30 ppm, while the methine proton appears at 4.10–4.18 ppm. After reacting with Au(III), gold particles in the solution could be visualized with the naked eye. Two new peaks appeared at 3.10 and 4.03 ppm in the ¹H NMR spectra after 1 min. The methylene and methine protons of cysteine appeared at 2.89–3.02 ppm and 4.01–4.10 ppm, respectively, both signals shifted slightly upfield relative to cystine. During the complexation of cysteine with Au(III), precipitation was immediately formed in the solution. After one minute of exposure to Au(III), neither of the original cysteine signals remained. After 1 h of contact with Au(III), the same two new peaks observed for cystine are visible for cysteine.

Because the reduction of the dimer cystine to monomer cysteine appears to have taken place alongside the reduction from Au(III) to metallic Au, the details of this transformation will be considered. In the initial step, cystine would undergo hydrolysis in acidic aqueous solution to form cysteine. Cysteine would then be oxidized back to cystine alongside the reduction of Au(III) to metallic Au. We have demonstrated that cysteine can be partially oxidized by hydrogen peroxide to form cystine (Fig. S4). We therefore propose that Au(III), acting similarly to hydrogen peroxide, also oxidizes this transformation. This rapid sequence of reactions leads to the observation of the same peaks for cystine and cysteine after 1 h contact with Au(III). Note that the complexation with Au(III) results in signals distinct from the original signals of free cystine and cysteine. While insight into the mechanism of the complexation of gold with cystine and cysteine has been achieved, the precise mechanism remains complex.

3.7. The proposed adsorption model

Precise understanding of the adsorption model is complicated by the fact that many reactions take place simultaneously. We propose the following sequence to explain the adsorption observed: Firstly, HH are treated with acidic solution and release cystine or cysteine from inner layers. Cystine is hydrolyzed or reduced to cysteine. The newly formed cysteine is then readily oxidized back to cystine by the reduction of Au(III) to metallic gold. These reactions are rapid and all take place within a minute. Complexation and coordination of Au(III) with sulfur atoms in cystine and cysteine may also take place. Plausible reactions contributing to this adsorption model are detailed below:

$$R\text{-}S\text{-}S\text{-}R + 2H_2O \rightarrow 2R\text{-}S\text{-}H + 2OH^- \ (\text{Hydrolysis}), \tag{7}$$

$$R\text{-}S\text{-}S\text{-}R + 2H^+ + 2e^- \rightarrow 2R\text{-}SH \ (\text{Reduction}) \tag{8}$$

$$2R\text{-}SH \rightarrow R\text{-}S\text{-}S\text{-}R + 2H^+ + 2e^- \ (\text{Oxidation}) \tag{9}$$

$$Au^{3+} + 3e^- \rightarrow Au^0 \ (\text{Reduction}) \tag{10}$$

$$2R\text{-}SH + Au^{3+} \rightleftarrows [(R\text{-}S)_2\text{-}Au]^+ + 2H^+ \ (\text{Complexation}) \tag{11}$$

$$4R\text{-}SH + Au^{3+} \rightleftarrows [(R\text{-}S)_4\text{-}Au]^- + 4H^+ \ (\text{Complexation}) \tag{12}$$

Scheme 1. Proposed scheme of Au(III) adsorption processes on human hair.
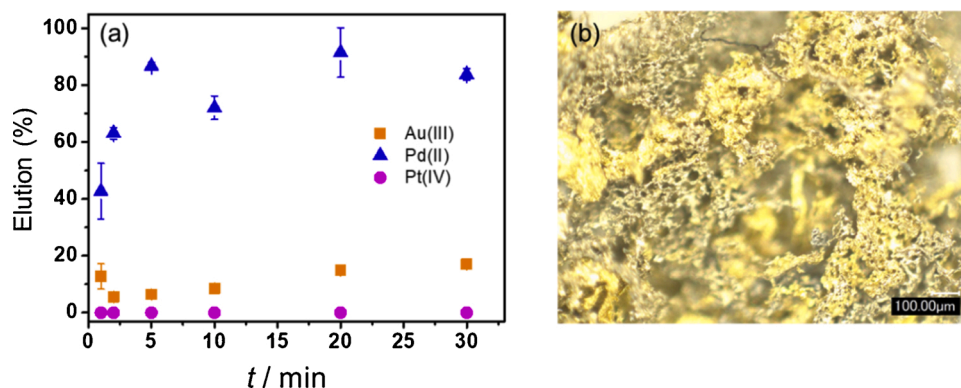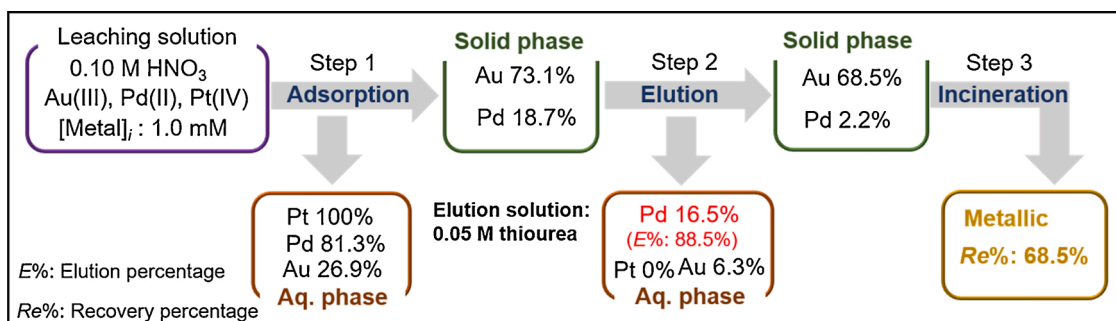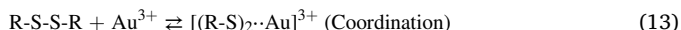
Fig. 8. (a) Recovery of precious metals from HH with acidic thiourea, (b) microscope image of the pure and filamentous metallic gold obtained from incineration.

Scheme 2. Stepwise recovery of metallic gold from mixed precious metal solution with human hair.

and

$$R\text{-}S\text{-}S\text{-}R + Au^{3+} \rightleftarrows [(R\text{-}S)_2 \cdot\cdot Au]^{3+} \text{ (Coordination)} \quad (13)$$

The adsorption process is detailed in Scheme 1. Notably, the redox potential of the conversion of Au(III) to Au(0) is much higher than Pt(IV) to Pt(0) and Pd(II) to Pd(0). [45] This may explain why adsorption on HH and subsequent reduction was achieved for only Au(III).

3.8. Selective recovery of gold after competitive adsorption

The excellent selectivity of HH for Au(III) adsorption demonstrated in the competitive system increases the feasibility that this new bio-adsorbent could be applied in the processing of real waste leaching solutions. To further support potential future applications, the selective recovery of gold after competitive adsorption was investigated. HH loaded with precious metals was washed with acidic thiourea (0.05 M in 0.01 M HCl). The time dependence of the elution percentage is shown in Fig. 8a. Because very little Pt(IV) was initially adsorbed by HH, the elution percentage of Pt(IV) was negligible. The elution percentage of Au with acidic thiourea was also very modest, while Pd(II) was eluted most successfully. Because the loading capacity of Pd(II) on HH was also extremely small, the elution of the co-loaded-Pd(II) with acidic thiourea for 5 min was determined to be sufficiently effective. After the elution of Pd(II), the pure metallic gold remaining in the HH was recovered using incineration in a muffle furnace. The microscope image of the pure and filamentous metallic gold after incineration is shown in Fig. 8b. Thus, the recovery of pure gold can be achieved with a simple stepwise process requiring only adsorption, washing with acidic thiourea and finally recovery with incineration, as shown in Scheme 2. Untreated HH is a promising bio-adsorbent for the selective purification and recovery of gold over other precious metals.

4. Conclusions

An advanced technique for the recovery of gold using natural biomass waste was studied. Untreated HH waste exhibited high adsorptive selectivity and adsorption capacity for gold among other precious metals. Melanin as hair pigment was unrelated to gold adsorption. L-Cystine and L-cysteine were the main components responsible for gold adsorption and reduction supported by ^{1}H NMR studies. Pure gold was recovered from solution containing other metals by adsorption using HH, followed by wash and incineration. Nature HH waste is chemically stable and can be an abundant bio-adsorbent used to achieve specific selectivity and excellent adsorption without any chemical modification.

author-services.edanzgroup.com/) for editing a draft of this manuscript. The XRD measurements were conducted at Analytical Research Center for Experimental Sciences, Saga University.

Appendix A. Supplementary data

Supplementary material related to this article can be found, in the online version, at doi:https://doi.org/10.1016/j.jece.2020.104724.

References

[1] C.P. Baldé, V. Forti, V. Gray, R. Kuehr, P. Stegmann, The global E-waste monitor - 2017, United Nations Univerisy (UNU), International Telecommunication Union (ITU) & International Solid Waste Association (ISWA), Boon/ Geneva/Vienna.

[2] A. Fornalczyk, M. Saternus, Platinum recovery from used auto catalytic converts in electrorefining process, Metalurgija 52 (2013) 219–222.

[3] A. Fornalczyk, J. Willner, K. Francuz, J. Cebulski, E-waste as a source of valuable metals, Arch. Mater. Sci. Eng. 63 (2013) 87–92.

[4] G. Chauhan, P.R. Jadhao, K.K. Pant, K.D.P. Nigam, Novel technologies and conventional processes for recovery of metals from waste electrical and electronic equipment: challenges & opportunities-A review, J. Environ. Chem. Eng. 6 (2018) 1288–1304, https://doi.org/10.1016/j.jece.2018.01.032.

[5] J. Liu, H. Xu, L. Zhang, C.T. Liu, Economic and environmental feasibility of hydrometallurgical process for recycling waste mobile phones, Waste Manage. 111 (2020) 41–50, https://doi.org/10.1016/j.wasman.2020.05.017.

[6] J. Cui, L. Zhang, Metallurgical recovery of metals from electronic waste: a review, J. Hazard. Mater. 158 (2008) 228–256, https://doi.org/10.1016/j.jhazmat.2008.02.001.

[7] N.P. Shetti, D.S. Nayak, G.T. Kuchinad, Electrochemical oxidation of erythrosine at TiO₂ nanoparticles modified gold electrode – an environmental application, J. Environ. Chem. Eng. 5 (2017) 2083–2089, https://doi.org/10.1016/j.jece.2017.03.040.

[8] D.T. Sun, N. Gasilova, S.L. Yang, E. Oveisi, W.L. Queen, Rapid, selective extraction of trace amounts of gold from complex water mixtures with a metal-organic framework (MOF)/polymer composite, J. Am. Chem. Soc. 140 (2018) 16697–16703, https://doi.org/10.1021/jacs.8b09555.

[9] B.T. Khogare, G.S. Kamble, A.N. Kokare, S.B. Zanje, V.J. Suryavanshi, M.A. Anuse, P.B. Piste, B.N. Kokare, Development of novel solvent extraction method for determination of gold(III) using 4-heptylaminopyridine: application to alloys and environmental analysis, J. Environ. Chem. Eng. 4 (2016) 3075–3083, https://doi.org/10.1016/j.jece.2016.06.001.

[10] A.G. Ghomi, N. Asasian-Kolur, S. Sharifian, A. Golnaraghi, Biosorption for sustainable recovery of precious metals from wastewater, J. Environ. Chem. Eng. 8 (2020) 103996, https://doi.org/10.1016/j.jece.2020.103996.

[11] B.C. Choudhary, D. Paul, A. Borse, D.J. Garole, Recovery of palladium from secondary waste using soluble tannins crosslinked Lagerstroemia speciosa leaves powder, J. Chem. Technol. Biotechnol. 92 (2017) 1667–1677, https://doi.org/10.1002/jctb.5163.

[12] J.S. Lim, S.M. Kim, S.Y. Lee, E.A. Stach, J.N. Culver, M.T. Harris, Quantitative study of Au(III) and Pd(II) ion biosorption on genetically engineered tobacco mosaic virus, J. Colloid Interf. Sci. 342 (2019) 455–461, https://doi.org/10.1016/j.jcis.2009.10.028.

[13] M.-H. Song, J.A. Kim, W. Wei, S. Kim, Y.-S. Yun, Polyethylenimine-coated biomass-chitosan composite fibers for recovery of ruthenium from industrial effluent: Effects of chitosan molecular weight and drying method, Hydrometallurgy 182 (2018) 114–120, https://doi.org/10.1016/j.hydromet.2018.11.001.

[14] T. Maruyama, H. Matsushita, Y. Shimada, I. Kamata, M. Hanaki, S. Sonokawa, N. Kamiya, M. Goto, Proteins and protein-rich biomass as environmentally friendly adsorbents selective for precious metal ions, Environ. Sci. Technol. 41 (2007) 1359–1364, https://doi.org/10.1021/es061664x.

[15] J.K. Bediako, J.W. Choi, M.H. Song, Y. Zhao, S. Lin, A.K. Sarkar, C.-W. Cho, Y.-S. Yun, Recovery of gold via adsorption-incineration techniques using banana peel and its derivatives: selectivity and mechanisms, Waste Manage. 113 (2020) 225–235, https://doi.org/10.1016/j.wasman.2020.05.053.

[16] A. Gupta, Human hair "waste" and its utilization: gaps and possibilities, J. Waste Manag. (2014), https://doi.org/10.1155/2014/498018.

[17] World Population Prospects-Population Division-United Nations, http://population.un.org/wpp/Download/Standard/population.

[18] C.R. Robbins, Chemical and Physical Behavior of Human Hair, 3rd ed., Springer-Verlag, 1994, pp. 10–391.

[19] A. Nakamura, M. Arimoto, K. Takeuchi, T. Fujii, A rapid extraction procedure of human hair proteins and identification of phosphorylated species, Biol. Pharm. Bull. 25 (2002) 569–572, https://doi.org/10.1248/bpb.25.569.

[20] X.H. Xu, B. Bai, H.L. Wang, Y.R. Suo, Synthesis of human hair fiber-impregnated chitosan beads functionalized with citric acid for the adsorption of lysozyme, RSC Adv. 7 (2017) 6636–6647, https://doi.org/10.1039/C6RA26542A.

[21] S. Shin, A. Lee, S. Lee, K. Lee, J. Kwon, M.Y. Yoon, J. Hong, D. Lee, G.H. Lee, J. Kim, Microwave-assisted extraction of human hair proteins, Anal. Biochem. 407 (2010) 281–283, https://doi.org/10.1016/j.ab.2010.08021.

[22] A. Kuzuhara, Analysis of structural changes in bleached keratin fibers (black and white human hair) using Raman spectroscopy, Biopolymers 81 (2006) 506–514, https://doi.org/10.1002/bip.20453.

[23] C.R. Robbins, C.H. Kelly, Amino acid composition of human hair, Text. Res. J. 40 (1970) 891–896, https://doi.org/10.1177/004051757004001005.

[24] R.G. Pearson, Hard and soft acids and bases, J. Am. Chem. Soc. 85 (1963) 3533–3539, https://doi.org/10.1021/ja00905a001.

[25] R.G. Pearson, J. Songstad, Application of the principle of hard soft acids and bases to organic chemistry, J. Am. Chem. Soc. 89 (1967) 1827–1836, https://doi.org/10.1021/ja00984a014.

[26] Z.F. Ma, H.L. Han, One-step synthesis of cystine-coated gold nanoparticles in aqueous solution, Colloids Surf. A: Physicochem. Eng. Aspects 317 (2008) 229–233, https://doi.org/10.1016/j.colsurfa.2007.10.018.

[27] J.D. Zhang, Q.J. Chi, J.U. Nielsen, E.P. Friis, J.E.T. Andersen, J. Ulstrup, Two-dimensional cysteine and cystine cluster networks on Au(111) disclosed by voltammetry and in situ scanning tunneling microscopy, Langmuir 16 (2000) 7229–7237, https://doi.org/10.1021/la000246h.

[28] L.G. Sillén, A.E. Martell, J. Bjerrum, Stability constants of metal-ion complexes, Special publication, Royal Soc. Chem. 17 (1964) 288–289.

[29] M.J. Nicol, C.A. Fleming, R.L. Paul, The Chemistry of the Extraction of Gold, Chapter 15, 1987, pp. 831–905.

[30] I. Langmuir, The constitution and fundamental properties of solids and liquids. II. liquids1, J. Am. Chem. Soc. 39 (1917) 1848–1906, https://doi.org/10.1021/ja02254a006.

[31] X.Q. Chen, K.F. Lam, S.F. Mak, K.L. Yeung, Precious metal recovery by selective adsorption using biosorbents, J. Hazard. Mater. 186 (2011) 902–910, https://doi.org/10.1016/j.jhazmat.2010.11.088.

[32] S.I. Ishikawa, K. Suyama, K. Arihara, M. Itoh, Uptake and recovery of gold ions from electroplating wastes using eggshell membrane, Bioresour. Technol. 81 (2002) 201–206, https://doi.org/10.1016/S0960-8524(01)00134-1.

[33] B.C. Choudhary, D. Paul, A.U. Borse, D.J. Garole, Surface functionalized biomass for adsorption and recovery of gold from electronic scrap and refinery wastewater, Sep. Purif. Technol. 195 (2018) 260–270, https://doi.org/10.1016/j.seppur.2017.12.024.

[34] A.D. Dwivedi, S.P. Dubey, S. Hokkanen, R.N. Fallah, M. Sillanpää, Recovery of gold from aqueous solutions by taurine modified cellulose: An adsorptive reduction pathway, Chem. Eng. J. 255 (2014) 97–106, https://doi.org/10.1016/j.cej.2014.06.017.

[35] H.M. Al-Saidi, The fast recovery of gold(III) ions from aqueous solutions using raw date pits: kinetic, thermodynamic and equilibrium studies, J. Saudi. Chem. Soc. 20 (2016) 615–624, https://doi.org/10.1016/j.jscs.2013.06.002.

[36] D. Parajuli, K. Hirota, K. Inoue, Trimethylamine-modified lignophenol for the recovery of precious metals, Ind. Eng. Chem. Res. 48 (2009) 10163–10168, https://doi.org/10.1021/ie801829w.

[37] E. Torres, Y.N. Mata, M.L. Blázquez, J.A. Muñoz, F. González, A. Ballester, Gold and silver uptake and nanoprecipitation on calcium alginate beads, Langmuir 21 (2005) 7951–7958, https://doi.org/10.1021/la046852k.

[38] D. Parajuli, C.R. Adhikari, M. Kuriyama, H. Kawakita, K. Ohto, K. Inoue, M. Funaoka, Selective recovery of gold by novel lignin-based adsorption gels, Ind. Eng. Chem. Res. 45 (2006) 8–14, https://doi.org/10.1021/ie050532u.

[39] D. Parajuli, H. Kawakita, K. Inoue, K. Ohto, K. Kajiyama, Persimmon peel gel for the selective recovery of gold, Hydrometallurgy 87 (2007) 133–139, https://doi.org/10.1016/j.hydromet.2007.02.006.

[40] D. Parajuli, C.R. Adhikari, H. Kawakita, S. Yamada, K. Ohto, K. Inoue, Chestnut pellicle for the recovery of gold, Bioresour. Technol. 100 (2008) 1000–1002, https://doi.org /10.1016/j.biortech.2008.06.058.

[41] B. Pangeni, H. Paudyal, M. Abe, K. Inoue, H. Kawakita, K. Ohto, B.B. Adhikari, S. Alam, Selective recovery of gold using some cross-linked polysaccharide gels, Green Chem. 14 (2012) 1917–1927, https://doi.org /10.1039/C2GC35321K.

[42] K. Inoue, M. Gurung, H. Kawakita, K. Ohto, D. Parajuli, B. Pangeni, S. Alam, in: S. Sabir (Ed.), The Recovery of Gold from Secondary Sources, World Scientific Publishing Co. Ltd., Chapter 5, 2016, pp. 143–171, https://doi.org /10.3390/ma10080857.

[43] S. Krishnamurthy, A. Esterle, N.C. Sharma, S.V. Sahi, Yucca-derived synthesis of gold nanomaterial and their catalytic potential, Nanoscale Res. Lett. 9 (2014) 627. http://www.nanoscalereslett.com/content/9/1/627.

[44] K. Selvan, S. Rajan, T. Suganya, G. Parameshwari, M. Antonysamy, Immunocosmeceuticals: an emerging trend in repairing human hair damage, Chron. Young Sci. 4 (2013) 81–85, https://doi.org/10.4103/2229-5186.115531.

[45] K. Shimura, H. Yoshida, Haterogeneous photocatalytic hydrogen production from water and biomass derivatives, Energy Environ. Sci. 4 (2011) 2467–2481, https://doi.org/10.1039/C1EE01120K.